Crooks equation for steered molecular dynamics using a Nosé-Hoover thermostat

Piero Procacci, Simone Marsili, Alessandro Barducci, Giorgio F. Signorini, and Riccardo Chelli

Citation: J. Chem. Phys. **125**, 164101 (2006); doi: 10.1063/1.2360273
View online: http://dx.doi.org/10.1063/1.2360273
View Table of Contents: http://jcp.aip.org/resource/1/JCPSA6/v125/i16
Published by the American Institute of Physics.

Additional information on J. Chem. Phys.

Journal Homepage: http://jcp.aip.org/
Journal Information: http://jcp.aip.org/about/about_the_journal
Top downloads: http://jcp.aip.org/features/most_downloaded
Information for Authors: http://jcp.aip.org/authors

ADVERTISEMENT

Downloaded 12 Nov 2012 to 150.217.154.21. Redistribution subject to AIP license or copyright; see http://jcp.aip.org/about/rights_and_permissions

Crooks equation for steered molecular dynamics using a Nosé-Hoover thermostat

Piero Procacci[a)]
Dipartimento di Chimica, Università di Firenze, Via della Lastruccia 3, I-50019 Sesto Fiorentino, Italy and European Laboratory for Non-linear Spectroscopy (LENS), Via Nello Carrara 1, I-50019 Sesto Fiorentino, Italy

Simone Marsili, Alessandro Barducci, and Giorgio F. Signorini
Dipartimento di Chimica, Università di Firenze, Via della Lastruccia 3, I-50019 Sesto Fiorentino, Italy

Riccardo Chelli
Dipartimento di Chimica, Università di Firenze, Via della Lastruccia 3, I-50019 Sesto Fiorentino, Italy; European Laboratory for Non-linear Spectroscopy (LENS), Via Nello Carrara 1, I-50019 Sesto Fiorentino, Italy; and Consorzio Interuniversitario Nazionale per la Scienza e Tecnologia dei Materiali (INSTM), I-50121 Firenze, Italy

(Received 17 March 2006; accepted 13 September 2006; published online 23 October 2006)

The Crooks equation [Eq. (10) in J. Stat. Phys. **90**, 1481 (1998)], originally derived for microscopically reversible Markovian systems, relates the work done on a system during an irreversible transformation to the free energy difference between the final and the initial state of the transformation. In the present work we provide a theoretical proof of the Crooks equation in the context of constant volume, constant temperature steered molecular dynamics simulations of systems thermostated by means of the Nosé-Hoover method (and its variant using a chain of thermostats). As a numerical test we use the folding and unfolding processes of decaalanine *in vacuo* at finite temperature. We show that the distribution of the irreversible work for the folding process is markedly non-Gaussian thereby implying, according to Crooks equation, that also the work distribution of the unfolding process must be inherently non-Gaussian. The clearly asymmetric behavior of the forward and backward irreversible work distributions is a signature of a non-Markovian regime for the folding/unfolding of decaalanine. © *2006 American Institute of Physics*. [DOI: 10.1063/1.2360273]

I. INTRODUCTION

Among the methods devised for calculating free energy surfaces, the Jarzynski equality[1,2] (JE) and the correlated Crooks equation[3] (CE) are perhaps some of the most intriguing because of their far reaching theoretical implications. In fact, they establish a strict correlation between two seemingly unrelated physical quantities, i.e., the work done on a system during irreversible (or better, dissipative) transformations and the free energy difference between the final and the initial state of the transformations.[4] According to Crooks,[3] JE appears to follow from a more general equation (that we will refer to as CE), that is Eq. (10) of Ref. 3 [see also Eq. (2) of the present paper]. The CE is, in fact, a point by point relation involving statistical distributions of the work, while the JE regards average values. If, on the one side, the JE appears to be less general than the CE, on the other side it was derived using more general assumptions with respect to CE. The JE is indeed essentially based on the canonical distribution (i.e., the basic statistical postulate) and on the Liouville theorem.[1,5] The CE, in its original formulation, is instead based on the microscopic reversibility and on the Markov chain assumption used, e.g., in Monte Carlo simulations.[6] Crooks himself made a step forward generalizing the equation to dynamical Markovian systems[7] (e.g., those obeying the overdamped Langevin equation). More recently, Evans,[8] starting from the transient fluctuation theorem,[9] demonstrated the CE for general (not necessarily Markovian) dynamical systems in the isokinetic thermodynamical ensemble.

From the experimental point of view, both the JE (Ref. 10) and, more recently, CE (Ref. 11) have been verified using atomic force microscopy. However, as pointed out by several authors,[11–13] these experiments have been all conducted in conditions in which the system is close to equilibrium with Gaussian or nearly Gaussian fluctuations around the mean dissipated work.[12]

Recently Park and Schulten[14] have performed extensive computer experiments using steered molecular dynamics (SMD) simulations on decaalanine aimed at numerically verifying the JE and CE. In agreement with early studies,[15,16] Park and Schulten showed the statistical difficulties of estimating the free energy along the unfolding coordinate by using the JE. Nonetheless, in the forced unfolding of the α-helix form of decaalanine, they obtained seemingly Gaussian work distributions. The Gaussian shape of the work distribution was put forward as an evidence of the Markovian nature of the unfolding process. As remarked in several

[a)]Author to whom correspondence should be addressed. Electronic mail: procacci@chim.unifi.it

 © 2006 American Institute of Physics

Downloaded 12 Nov 2012 to 150.217.154.21. Redistribution subject to AIP license or copyright; see http://jcp.aip.org/about/rights_and_permissions

studies,[12,14,15,17] when the work distribution in the one direction, $P_f(W)$, is Gaussian, then the CE sets strict constraints for the work distribution of the backward transformation, $P_b(-W)$. In particular, if $P_f(W)$ is Gaussian, then (i) $P_b(-W)$ must also be Gaussian with identical width; (ii) the intersection point of $P_b(-W)$ and $P_f(W)$ falls at $W=\Delta F$, ΔF being the free energy difference for the forward transformation; (iii) the average work in the forward transformation $\bar{W}$, the variance σ of the work distributions, and the free energy difference ΔF obey the equation[15,17]

$$\bar{W} = \Delta F - \frac{\sigma^2}{2k_B T}. \tag{1}$$

Applying Eq. (1), Park and Schulten[14] found quite contradictory results. On the one hand, their SMD simulations provided almost perfect Gaussian work distributions for two very different steering velocities. On the other hand, the free energy curve calculated using the CE at the greatest steering velocity differs from the exact curve by about 20% (in the final state of the transformation). These results put some doubts either on the validity of the CE in the context of SMD simulations or on the Gaussian (and hence Markovian) nature of the unfolding transformation. Park and Schulten did not calculate the work distribution in the backward direction (refolding process) and hence they did not fully test the CE.

In the present work we derive the CE for a general system, whether Markovian or non-Markovian, for which the irreversible transformation is performed by SMD simulations with stiff spring approximation and the temperature is kept fixed with a Nosé-Hoover (NH) thermostat.[18,19] We also derive the CE when a chain of NH thermostats[20,21] is considered. In a recent article[22] Jarzynski proved that the CE is valid in the context of a procedure where the initial microstates for the forward and backward transformations are taken from canonical distributions, and the transformation is performed removing the heat reservoir. The Jarzynski's proof follows straightforwardly from our demonstration by simply setting the mass of the thermostat to infinity during the transformation, that is, removing the heat exchange between system and thermal bath.

While this paper was under review, Cuendet published a statistical mechanical route to the JE based on the equations of motions for the non-Hamiltonian NH dynamics.[23] In our derivation of the CE we use basically the strategy of Cuendet based on the equations of motions. In this sense our study can be considered as an extension of Cuendet's work. The main difference between our derivation of the CE and the Cuendet's demonstration of the JE consists in the initial step of the proof. In our case the starting point is the fluctuation theorem[9] that holds for a single transformation (and its time reversal), while in Ref. 23 the starting point is the ensemble average of the exponential of the work done during a transformation. From this second point of view, since JE can be trivially derived from the CE but not vice versa, the Cuendet's derivation can be considered less general.

Extended numerical tests are also performed. As exemplary system we have considered the widely studied process of helix-coil folding of decaalanine *in vacuo* at finite temperature.[14,24] We have found that the two work distributions, $P_f(W)$ and $P_b(-W)$, indeed obey the CE, irrespective of the steering velocity. In addition, contrary to what is generally assumed,[14,17] we have verified that, in the specific case of decaalanine, the work distributions are inherently non-Gaussian. Since a Gaussian work distribution is generated when the process is Markovian,[14] the non-Gaussian shape we observe for the refolding transformation, far from disproving the CE, could provide additional information on the dynamical regime of decaalanine, indicating a finite damping behavior along the folding/unfolding reaction coordinate.

The outline of the article is as follows. In Sec. II we provide the theory. In Sec. III we report numerical tests. Conclusive remarks are given in Sec. IV.

II. THEORY

A. Crooks equation

The CE has been originally derived[3] for microscopically reversible Markovian systems in the context of Monte Carlo simulations.[6] If we define a generic reaction coordinate as a function of the Cartesian coordinates of the particles of a system (e.g., a distance between two atoms or a torsional angle), we can characterize every point along the reaction coordinate path by a parameter λ, such that $\lambda=0$ and $\lambda=1$ correspond to two ensembles of microstates (from now on indicated as macrostates $\mathcal{A}$ and $\mathcal{B}$, respectively) for which the reaction coordinate is constrained to different values. A dynamical process where λ is externally driven from 0 to 1, according to an arbitrary time scheduling, will be referred as *forward* transformation, while the time-reversal path will be indicated as *backward* transformation. Given these definitions, the CE sets a relation between the following four quantities.

(1) $P(A \to B)$, i.e., the joint probability of taking a microstate A from the macrostate $\mathcal{A}$ (through a canonical sampling) and of performing the forward transformation to the microstate B belonging to the macrostate $\mathcal{B}$.
(2) $P(A \leftarrow B)$, i.e., the joint probability of taking the microstate B from the macrostate $\mathcal{B}$ (through a canonical sampling) and performing the backward transformation to the microstate A.
(3) W_{AB}, i.e., the work done on the system during the forward transformation (from A to B).
(4) $\Delta F = F(\mathcal{B}) - F(\mathcal{A})$, i.e., the free energy difference between the macrostates $\mathcal{A}$ and $\mathcal{B}$.

The CE reads as follows:

$$\frac{P(A \to B)}{P(A \leftarrow B)} = \exp[\beta(W_{AB} - \Delta F)], \tag{2}$$

where $\beta=(k_B T)^{-1}$, k_B being the Boltzmann constant, and T the temperature. In the previous equation the difference $W_{AB}-\Delta F$ corresponds to the work dissipated in the forward transformation. Using the relation $W_{AB}=-W_{BA}$ (where W_{BA} is the work done on the system in the backward transformation), and grouping together all the trajectories yielding the same work (in the forward and backward transformation), the following relation can be recovered:[25]

Downloaded 12 Nov 2012 to 150.217.154.21. Redistribution subject to AIP license or copyright; see http://jcp.aip.org/about/rights_and_permissions

$$P_{\mathcal{A}\to\mathcal{B}}(W) = P_{\mathcal{A}\leftarrow\mathcal{B}}(-W)\exp[\beta(W-\Delta F)], \tag{3}$$

where $P_{\mathcal{A}\to\mathcal{B}}(W)$ and $P_{\mathcal{A}\leftarrow\mathcal{B}}(-W)$ are the work distribution functions obtained from the forward and backward transformations, respectively. Here W is intended to be the work done on the system in the forward transformation.

B. Crooks equation: Shape of the work distributions for Markovian systems

As stated in the Introduction, Eq. (2) sets strong limitations to the behavior of the forward and backward work distributions [Eq. (3)]. In particular, since $\int P_{\mathcal{A}\to\mathcal{B}}(W)dW=1$, $P_{\mathcal{A}\leftarrow\mathcal{B}}(-W)$ will vanish for $W\to\infty$ at a faster rate than $\exp(-\beta W)$, so that the integrand function decays to zero. Correspondingly, since $\int P_{\mathcal{A}\leftarrow\mathcal{B}}(-W)dW=1$, $P_{\mathcal{A}\to\mathcal{B}}(W)$ will decay to zero faster than $\exp(\beta W)$ for $W\to-\infty$. A Gaussian distribution indeed satisfies this condition. In this respect, Park and Schulten showed[14] that, under the assumption that the system is Markovian, SMD simulations with stiff springs result in Gaussian work distributions. However, not all Gaussian distributions are allowed. In fact, Eq. (3) establishes a relation between the moments of the normal distribution (in particular, $\bar{W}$ and $\sigma^2=\overline{W^2}-\bar{W}^2$) and ΔF. Suppose that, for a given velocity of the forward transformations $\mathcal{A}\to\mathcal{B}$, the work distribution $P_{\mathcal{A}\to\mathcal{B}}(W)$ is a (normalized) Gaussian function.[14] Then, according to Eq. (3), we have that

$$P_{\mathcal{A}\leftarrow\mathcal{B}}(-W) = \frac{1}{\sigma\sqrt{2\pi}}\exp\left[\frac{-(W-\bar{W}_{\mathcal{A}\mathcal{B}})^2}{2\sigma^2}\right]\exp[\beta(\Delta F-W)], \tag{4}$$

where $\bar{W}_{\mathcal{A}\mathcal{B}}$ is the average work done on the system in the forward transformations $\mathcal{A}\to\mathcal{B}$. The above equation may be rearranged as follows:

$$P_{\mathcal{A}\leftarrow\mathcal{B}}(-W) = \frac{1}{\sigma\sqrt{2\pi}}\exp\left[\beta\left(\Delta F-\bar{W}_{\mathcal{A}\mathcal{B}}+\frac{\beta\sigma^2}{2}\right)\right] \times\exp\left[\frac{-(-W+\bar{W}_{\mathcal{A}\mathcal{B}}-\beta\sigma^2)^2}{2\sigma^2}\right]. \tag{5}$$

From the previous equation we conclude that $P_{\mathcal{A}\to\mathcal{B}}(W)$ and $P_{\mathcal{A}\leftarrow\mathcal{B}}(-W)$ are Gaussian functions with identical width. The center of $P_{\mathcal{A}\leftarrow\mathcal{B}}(-W)$ falls at $\bar{W}_{\mathcal{B}\mathcal{A}}=-\bar{W}_{\mathcal{A}\mathcal{B}}+\beta\sigma^2$. Moreover the intersection point of the two work distributions occurs at $W=\Delta F$. Considering that $P_{\mathcal{A}\leftarrow\mathcal{B}}(-W)$ must be normalized to one, the following equations hold

$$\Delta F = \bar{W}_{\mathcal{A}\mathcal{B}}-\frac{\beta\sigma^2}{2}, \tag{6}$$

$$\Delta F = -\bar{W}_{\mathcal{B}\mathcal{A}}+\frac{\beta\sigma^2}{2}. \tag{7}$$

Summing term by term Eqs. (6) and (7), we get[17]

$$\Delta F = \tfrac{1}{2}(\bar{W}_{\mathcal{A}\mathcal{B}}-\bar{W}_{\mathcal{B}\mathcal{A}}). \tag{8}$$

Equation (6) [or Eq. (7)] can in principle be used to recover the entire free energy of the system along the λ coordinate. Interestingly, if one of the forward or backward work distributions is not Gaussian then the other one cannot be Gaussian either. In such cases Eq. (8) could be used as an approximation. Alternatively, one could use directly Eq. (3) and histogram methods to calculate ΔF.

C. Crooks equation for SMD simulations using a Nosé-Hoover thermostat

In deriving the CE for the case of constant volume, constant temperature SMD simulations using a NH thermostat,[18,19] we start from considering the ratio between the probability of observing a given phase space trajectory from a microstate A to a microstate B, $p[A(\mathbf{x}(0))\to B(\mathbf{x}(\tau))]$, and the probability of observing the time-reversal trajectory, $p[A(\mathbf{x}(0))\leftarrow B(\mathbf{x}(\tau))]$:

$$\frac{p[A(\mathbf{x}(0))\to B(\mathbf{x}(\tau))]}{p[A(\mathbf{x}(0))\leftarrow B(\mathbf{x}(\tau))]} = \frac{p[A(\mathbf{x}(0))]}{p[B(\mathbf{x}(\tau))]}\exp\left(-\int_0^\tau \nabla_{\mathbf{x}}\cdot\dot{\mathbf{x}}\,dt\right), \tag{9}$$

where τ is the duration of the irreversible process, $\mathbf{x}$ is a vector in the multidimensional phase space, $p[A(\mathbf{x}(0))]$ and $p[B(\mathbf{x}(\tau))]$ are the probabilities (not necessarily at equilibrium) of the phase space points $\mathbf{x}(0)$ and $\mathbf{x}(\tau)$, respectively. The function $\nabla_{\mathbf{x}}\cdot\dot{\mathbf{x}}$ is the divergence of the phase space velocity, the so-called compressibility of the system.[26] Equation (9) was derived by Evans[9,27] and is extraordinarily general. In fact, it holds for both Hamiltonian and non-Hamiltonian systems with time-reversal invariant equation of motions. A proof of Eq. (9) in the case that $p[A(\mathbf{x}(0))]$ and $p[B(\mathbf{x}(\tau))]$ are equilibrium probabilities is given in Appendix A.

We now assume that in the time τ the system is driven from the microstate A, characterized by the reaction coordinate $\zeta_{\mathcal{A}}$, to the microstate B, characterized by the reaction coordinate $\zeta_{\mathcal{B}}$, using a time dependent harmonic potential,

$$V(\zeta(\mathbf{q}),t) = \frac{k}{2}\left[\zeta(\mathbf{q})-\zeta_{\mathcal{A}}+(\zeta_{\mathcal{A}}-\zeta_{\mathcal{B}})\frac{t}{\tau}\right]^2. \tag{10}$$

The functional form of this potential implies that the reaction coordinate evolves with constant velocity. However, since an explicit expression of $V(\zeta(\mathbf{q}),t)$ is not required in the following proof, the use of a more complex time scheduling function would not change the final result. We must consider that, when $V(\zeta(\mathbf{q}),t)$ is added to the Hamiltonian of the system, the thermal energy provided by the thermostat can flow not only from and to the physical system but also from and to the additional potential term. The total energy of this extended system (physical system plus guiding potential) at time t is

$$H(t) = H_0 + V(\zeta,t), \tag{11}$$

where H_0 is the total energy of the physical system (kinetic energy plus internal potential energy). In the previous equation (and in the following) the dependence on $\mathbf{q}$ of the reaction coordinate is omitted for simplicity of notation. The total energy change in the $A\to B$ transformation can thus be calculated as follows:

Downloaded 12 Nov 2012 to 150.217.154.21. Redistribution subject to AIP license or copyright; see http://jcp.aip.org/about/rights_and_permissions

$$Q_{AB} + W_{AB} = \int_0^\tau \dot{H}(t)\, dt = H(\tau) - H(0), \tag{12}$$

where Q_{AB} and W_{AB} are the heat entering the system and the work done on the system during the transformation, respectively. We remark that the only allowed heat flow from and to the system occurs through the thermostat. Moreover, since we are dealing with a constant volume system, the work done on the system can only be performed through the guiding potential $V(\zeta,t)$. Considering Eq. (11), the total time derivative of $H(t)$ is

$$\dot{H}(t) = \frac{\partial V(\zeta,t)}{\partial t} + \nabla_{\mathbf{x}} V(\zeta,t)\cdot\dot{\mathbf{x}} + \nabla_{\mathbf{x}} H_0 \cdot \dot{\mathbf{x}}. \tag{13}$$

Substituting Eq. (13) into Eq. (12) and taking into account that the work performed on the system in the $A \to B$ transformation is

$$W_{AB} = \int_0^\tau \frac{\partial V(\zeta,t)}{\partial t}\, dt, \tag{14}$$

we obtain

$$Q_{AB} = \int_0^\tau \nabla_{\mathbf{x}} H_0 \cdot \dot{\mathbf{x}}\, dt + \int_0^\tau \nabla_{\mathbf{x}} V(\zeta,t)\cdot\dot{\mathbf{x}}\, dt. \tag{15}$$

In this equation the integral involving H_0 corresponds to the heat provided by the thermostat to the physical system, while the other integral is the heat related to the guiding potential term. Equation (15) can be written as follows:

$$Q_{AB} = \int_0^\tau \sum_{i=1}^{3N} \left[\left(\frac{\partial H_0}{\partial q_i} + \frac{\partial V(\zeta,t)}{\partial q_i} \right) \dot{q}_i + \frac{\partial H_0}{\partial p_i} \dot{p}_i \right] dt, \tag{16}$$

where we have considered that $V(\zeta,t)$ does not depend explicitly on the momenta. Equation (16) can be rearranged using the equations of motion that in the case of a system with a NH thermostat and with the guiding potential $V(\zeta,t)$ are[18,19]

$$\begin{aligned} \dot{q}_i &= \frac{\partial H_0}{\partial p_i}, \\ \dot{p}_i &= -\frac{\partial H_0}{\partial q_i} - \frac{\partial V(\zeta,t)}{\partial q_i} - \dot{\eta} p_i, \\ \dot{\eta} &= \frac{p_\eta}{M_\eta}, \\ \dot{p}_\eta &= \sum_{i=1}^{3N} \frac{p_i^2}{m_i} - \frac{3N}{\beta}, \end{aligned} \tag{17}$$

where η and p_η are the thermostat variable and its conjugate momentum, respectively, and M_η is the related inertia factor. Using the equations of motion into Eq. (16), we obtain

$$Q_{AB} = -\frac{3N}{\beta}\int_0^\tau \dot{\eta}\, dt + \frac{p_\eta^2(0) - p_\eta^2(\tau)}{2M_\eta}. \tag{18}$$

For a system coupled to a NH thermostat the compressibility is[26]

$$\nabla_{\mathbf{x}} \cdot \dot{\mathbf{x}} = -3N\dot{\eta}. \tag{19}$$

Substituting Eq. (19) into Eq. (18) we get

$$\int_0^\tau \nabla_{\mathbf{x}} \cdot \dot{\mathbf{x}}\, dt = \beta Q_{AB} + \beta \frac{p_\eta^2(\tau) - p_\eta^2(0)}{2M_\eta}. \tag{20}$$

The next ingredient needed in Eq. (9) is the ratio between the equilibrium probabilities $p[A(\mathbf{x}(0))]$ and $p[B(\mathbf{x}(\tau))]$. To this aim we note that for a system coupled to a NH thermostat, the $6N$-dimensional phase space ($3N$ particle coordinates and $3N$ conjugate momenta) is augmented by the two degrees of freedom of the thermostat, i.e., $\mathbf{x} = (\mathbf{q}, \mathbf{p}, \eta, \mathbf{p}_\eta)$. The ratio of the equilibrium probabilities of the microstates A and B is given by[18,26]

$$\begin{aligned} \frac{p[A(\mathbf{x}(0))]}{p[B(\mathbf{x}(\tau))]} &= \exp\left[\beta \frac{p_\eta^2(\tau) - p_\eta^2(0)}{2M_\eta} \right] \\ &\times \exp[\beta(H(\tau) - H(0) - \Delta F)], \end{aligned} \tag{21}$$

where $H(0)$ is the energy of the physical system plus the guiding potential energy in the microstate A [Eq. (11)]. $H(\tau)$ is the same quantity for the microstate B. Before proceeding, we remark that in Eq. (21) $\Delta F = F(\zeta=\zeta_{\mathcal{B}}) - F(\zeta=\zeta_{\mathcal{A}}) \equiv F(\mathcal{B}) - F(\mathcal{A})$ refers to equilibrium states whose Hamiltonian includes also the harmonic potential at fixed reaction coordinates $\zeta(0) \equiv \zeta_{\mathcal{A}}$ and $\zeta(\tau) \equiv \zeta_{\mathcal{B}}$. Our target would be that of getting free energy differences along the reaction coordinate for a system whose Hamiltonian includes *only* the kinetic energy of the particles and the real interparticle potential energy. In this respect, Park and Schulten[14] have shown that the free energy $F(\zeta)$ of a guided system becomes identical to the true free energy of the system in the stiff spring approximation, that is, for an infinite force constant k [see Eq. (10)].

Exploiting Eqs. (12), (20), and (21) into Eq. (9), we obtain

$$\frac{p[A(\mathbf{x}(0)) \to B(\mathbf{x}(\tau))]}{p[A(\mathbf{x}(0)) \leftarrow B(\mathbf{x}(\tau))]} = \exp[\beta(W_{AB} - \Delta F)]. \tag{22}$$

Equation (22) is the central result of this paper. Such equation is identical to Eq. (2) (originally derived for Markovian systems) and it has been derived for all dynamical systems (Markovian and non Markovian) coupled to a NH thermostat. As can be seen in the Appendix B, the demonstration reported above can be straightforwardly extended to the context of SMD simulations where the temperature is kept fixed with a NH chain algorithm.[20,21]

III. NUMERICAL TESTS

As discussed in Sec. II B, CE guarantees that if the forward work distribution is Gaussian, then the backward work distribution must also be Gaussian. From the computational standpoint this fact is extremely important since it would give a practical way to compute the free energy along a

Downloaded 12 Nov 2012 to 150.217.154.21. Redistribution subject to AIP license or copyright; see http://jcp.aip.org/about/rights_and_permissions

reaction coordinate with the simple Eq. (6) [or Eq. (7)]. Gaussian work distributions were actually found in the context of SMD simulations,[14] for the limited but significant case[14,28,29] of the unfolding of decaalanine. It is remarkable that in Ref. 14 almost Gaussian work distributions were observed for two very different steering velocities, i.e., $v=10$ Å ns^{-1} and $v=100$ Å ns^{-1}. Nonetheless, application of Eq. (6) provided a very good estimate of the free energy curve only for $v=10$ Å ns^{-1}, whereas for $v=100$ Å ns^{-1} a significant divergence from the exact result[14] was found (mainly for large end-to-end distances). This observation raises some doubts about either the validity of the CE in the context of SMD simulations or about the Gaussian nature of the underlying distributions that indeed for the unfolding of decaalanine "look" Gaussian.[14] As we have theoretically proved the CE for NH molecular dynamics (Sec. II C), in order to shed further light on this issue, we have repeated the numerical experiment by Park and Schulten.[14] In particular, we have carried out SMD simulations of decaalanine at finite temperature, but focusing on both forward (unfolding) and backward (folding) trajectories.

The N atom of the *N*-terminus residue has been constrained to a fixed position, while the N atom of the *C*-terminus residue has been constrained to move along a given fixed direction. The reaction coordinate ζ is hence taken to be the distance between the N atoms of the two terminal amide groups. Therefore the guiding potential for SMD has the form of Eq. (10), where ζ_A and ζ_B are the initial and final values of the reaction coordinate and τ is the total (simulation) time of the transformation. In the present study we arbitrarily assume the stretching of decaalanine, that is, the evolution from an α-helix ($\zeta_A=15.5$ Å) to an elongated configuration ($\zeta_B=31.5$ Å), as the forward process. It should be noted that in general the end-to-end distance does not uniquely determine the configurational state of polypeptides. However, the equilibrium distribution at $\zeta_A=15.5$ Å corresponds to an ensemble of microstates tightly peaked around the α-helix structure, as for this end-to-end distance alternative structures are virtually impossible.[14,28] The same holds true for the final totally stretched state at $\zeta_B=31.5$ Å. So these two equilibrium ensembles are well determined and can be effectively sampled using relatively few microstates.

The force constant used for guiding the processes [Eq. (10)] is 800 kcal mol^{-1} Å^{-2}, which is about 100 times larger than that used in Ref. 14. This allows to minimize the possible negative impact of the stiff spring approximation[14] on the free energy calculation. The force field for decaalanine is taken from Ref. 30. The starting configurations of decaalanine for the forward and backward trajectories were randomly picked from standard molecular dynamics simulations of the molecule using a harmonic potential (force constant $k=800$ kcal mol^{-1} Å^{-2}) on the end-to-end distance. The equilibrium values of the end-to-end distance were fixed to 15.5 and 31.5 Å for generating the initial configurations of the forward and backward trajectories, respectively. Constant temperature in both molecular dynamics and SMD simulations was enforced using a NH thermostat[18,19] at the temperature of 300 K. The considered steering velocities, expressed as the simulation time τ, are 10, 20, 30, 50, 100, and 200 ps. For each steering regime we generated 10^4 forward trajectories and 10^4 backward trajectories. As we will show below, such a sampling allows the quantities considered in the present study to reach a good convergence. All calculations were done with the program ORAC,[31] properly modified for performing SMD simulations.

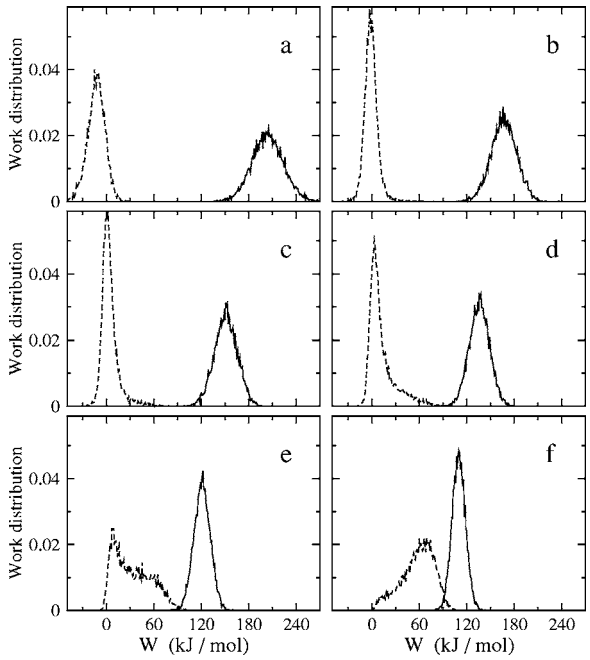

FIG. 1. $P_f(W)$ and $P_b(-W)$ work distribution functions (solid and dashed lines, respectively) for various steering velocities ($\tau=10$, 20, 30, 50, 100, and 200 ps from panel a to panel f).

In Fig. 1 we report the normalized work distributions $P_f(W)$ and $P_b(-W)$ for the forward and backward transformations, respectively. In agreement with Ref. 14, $P_f(W)$ indeed looks Gaussian for all steering velocities. On the contrary $P_b(-W)$ appears to deviate from the Gaussian trend for all steering regimes, the largest deviation occurring for the slower transformations ($\tau=100$ ps and $\tau=200$ ps). In order to quantify this observation, in Table I we report the first four moments of $P_f(W)$ and $P_b(-W)$. For a Gaussian function the expected values of s_3 and s_4 are zero, while from the table we see significant deviations from zero for both s_3 and s_4 at all steering regimes. In particular, while for $P_f(W)$ there is a general increase of the Gaussian character with the slowing down of the transformation, the $P_b(-W)$ distributions unexpectedly [see Eq. (5)] show the opposite behavior. Moreover we notice that the width of $P_f(W)$ differs significantly from that of $P_b(-W)$ at all steering velocities. Regarding the trends of the average values of the irreversible work ($\bar{W}_f$ and $-\bar{W}_b$ in Table I), we see that, as the process is slowed down, they tend to approach each other (see also Fig. 1) and will eventually become superimposed when the quasireversible regime is attained.

The large and unexpected difference between the work distribution functions in the forward and backward directions (see discussion above) could be related to incomplete statistical sampling. In order to show the statistical quality of our numerical tests, in Fig. 2 we report the $P_f(W)$ and $P_b(-W)$

Downloaded 12 Nov 2012 to 150.217.154.21. Redistribution subject to AIP license or copyright; see http://jcp.aip.org/about/rights_and_permissions

TABLE I. First four moments (in kJ mol^{-1}) of the work distributions for the forward $[P_f(W)]$ and backward $[P_b(-W)]$ transformations at various steering velocities.

	$P_f(W)$				$P_b(-W)$			
τ (ps)	$\bar{W}_f$	σ	s_3	s_4	$-\bar{W}_b$	σ	s_3	s_4
10	204.1	20.1	7.9	12.3	−13.1	11.3	7.6	9.6
20	167.5	16.2	5.9	8.3	−1.1	8.7	8.8	13.4
30	151.8	14.6	6.3	2.7	4.1	10.8	13.9	18.4
50	136.6	12.8	4.6	6.0	12.9	16.8	20.1	22.4
100	121.2	10.5	3.3	5.1	33.6	23.6	18.5	22.3
200	110.8	8.6	3.2	5.2	58.5	20.6	16.3	15.1

work distributions calculated for the steering velocity corresponding to $\tau=200$ ps using 10^4 and 2×10^3 trajectories. In spite of the large difference in terms of number of considered trajectories, the two sets of distributions are very similar except for the expected noise effects. The similarity of the work distributions calculated with different samplings is also confirmed numerically by the nearly coincidence of the four moments of the distributions (data not shown). This fact suggests that the non-Gaussian character of the backward work distributions has to be ascribed to the physics of the transformations, which in turn must be related to the non-Markovian character of the transformations themselves.

Although the work distributions reported in Fig. 1 are in general not Gaussian, we could tentatively use the equations for Gaussian distributions [Eqs. (6) and (7)] as done in Ref. 14, for reconstructing the potential of mean force, $F_f(\zeta)$, in the full interval spanned by the reaction coordinate. The free energy profile $F_f(\zeta)$ for the forward (unfolding) process is reported in Fig. 3 for the steering velocities corresponding to $\tau=20$ ps and $\tau=200$ ps. The exact free energy curve reported in Fig. 3 is calculated using the thermodynamic integration method. In order to show the amount of dissipated work along the reaction coordinate, we also provide the curve relative to the mean irreversible work. Comparing the mean irreversible work at the two steering velocities [Figs. 3(a) and 3(b)], we can appreciate the large dependence of the dissipated work on the steering regime. For $\tau=20$ ps, the mean irreversible work deviates from the exact free energy curve for all values of ζ. For $\tau=200$ ps we see instead that in the first stages of the transformation, i.e., for $15.5<\zeta<20$ Å, the mean irreversible work almost coincides with the exact free energy, implying a negligible dissipated work. The implications of this fact on $F_f(\zeta)$ are evident. At the lowest steering velocity the agreement between $F_f(\zeta)$ and the exact free energy is good, being less satisfactory for $\zeta>25$ Å. In general the faster the process, the larger the deviation of the Gaussian approximant $F_f(\zeta)$ from the exact free energy.

When we calculate the free energy using the data for the backward (folding) transformation [Figs. 3(c) and 3(d)], the agreement between the Gaussian approximant $F_b(\zeta)$ and the exact free energy profile becomes very unsatisfactory for both steering velocities. In particular, for the slowest quasireversible pulling [$\tau=200$ ps, Fig. 3(d)], the free energy difference $F_b(31.5)-F_b(15.5)$ surprisingly differs by as much as 30% from the exact value.

A summary of the performance of Eqs. (6) and (7) in the free energy estimate as a function of the steering regime is given in Fig. 4, where we report the free energy difference between the unfolded and folded states [$\Delta F=\Delta F_f=F_f(31.5)-F_f(15.5)$ for the forward transformation and $\Delta F=\Delta F_b$

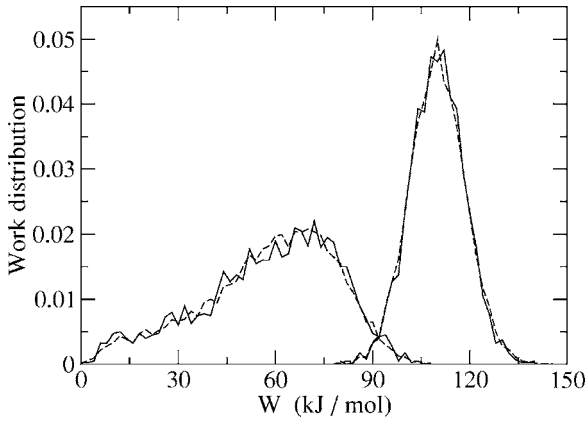

FIG. 2. $P_f(W)$ and $P_b(-W)$ work distribution functions (curves on the right and left parts of the graph, respectively) calculated for the slowest steering velocity ($\tau=200$ ps) using 10^4 and 2×10^3 trajectories (dashed and solid lines, respectively).

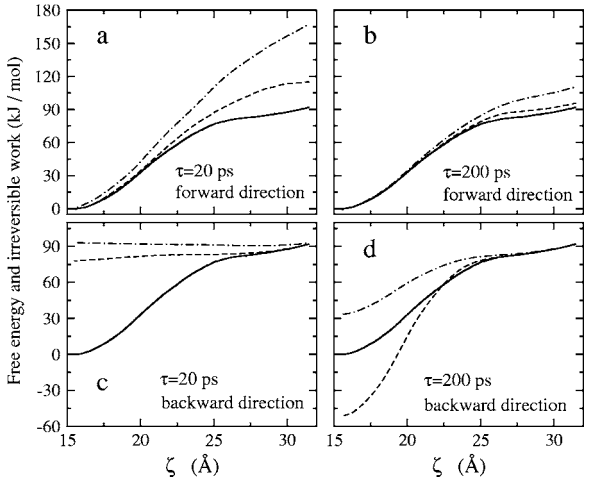

FIG. 3. Free energy and mean irreversible work as a function of the reaction coordinate ζ for the forward and backward transformations and two steering velocities. The exact free energy and the mean irreversible work are reported with solid and dot-dashed lines, respectively. The free energy $F_f(\zeta)$ for the forward direction (dashed lines in panels a and b) is calculated using Eq. (6). The free energy $F_b(\zeta)$ for the backward direction (dashed lines in panels c and d) is calculated using Eq. (7). Panel a: forward direction and $\tau=20$ ps; panel b: forward direction and $\tau=200$ ps; panel c: backward direction and $\tau=20$ ps; panel d: backward direction and $\tau=200$ ps.

Downloaded 12 Nov 2012 to 150.217.154.21. Redistribution subject to AIP license or copyright; see http://jcp.aip.org/about/rights_and_permissions

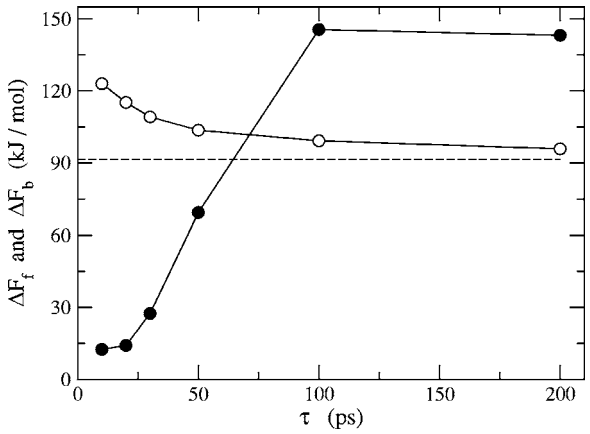

FIG. 4. Free energy difference of the unfolded and folded states of decaalanine as a function of the steering velocity (in terms of the simulation time τ). Open circles: ΔF_f calculated from the forward trajectories using Eq. (6). Full circles: ΔF_b calculated from the backward trajectories using Eq. (7). The horizontal dashed line indicates the exact ΔF calculated through thermodynamic integration. The lines are drawn as a guide for eyes.

$=F_b(31.5)-F_b(15.5)$ for the backward transformation]. ΔF_f is clearly convergent to the exact value with decreasing the steering velocity, whereas no clear trend can be extrapolated for ΔF_b.

These results reveal a striking asymmetry of the forward and backward transformations. In fact, assuming the validity of Eq. (5) in the case of Gaussian (or nearly Gaussian) work distributions, it remains completely unclear why $P_f(W)$ and $P_b(-W)$ are so different [relatively narrow and apparently Gaussian $P_f(W)$, broad and strongly asymmetric $P_b(-W)$] even for slow steering velocities. As a matter of fact, as stated in the first paragraph of this section, the validity of the CE implies that if one work distribution is Gaussian, then the work distribution relative to the inverse transformation must be Gaussian too. It seems therefore reasonable to assume that the same statement should hold true for *nearly* Gaussian work distributions. On the contrary, our results clearly indicate that a nearly Gaussian (Markovian) process in one direction can be markedly non-Gaussian in the reverse direction.

We may then try to calculate the free energy difference ΔF directly from Eq. (3), using exclusively $P_f(W)$ and $P_b(-W)$ making no assumption or approximation about their shape. According to Eq. (3), we note that ΔF corresponds exactly to the work, say, W_x, at which the intersection of $P_f(W)$ and $P_b(-W)$ occurs. For fast transformations this point falls on the tails of the work distributions (see Fig. 1) that are invariably the left tail of $P_f(W)$ and the right tail of $P_b(-W)$. From a computational standpoint, the determination of ΔF becomes more and more difficult with increasing mean dissipated work. If the steering velocity is too large, the two work distributions are far apart and W_x cannot be reliably determined [see Figs. 1(a)–1(d)]. For low steering velocity, W_x can instead be determined even quite precisely [Figs. 1(e) and 1(f)]. This scenario can be better appreciated in Fig. 5, where we report a zoomed view of Fig. 1. From the work distributions obtained at the two lowest steering velocities [Figs. 5(e) and 5(f)], we recover the almost exact ΔF. It is indeed remarkable that the estimate of ΔF using directly

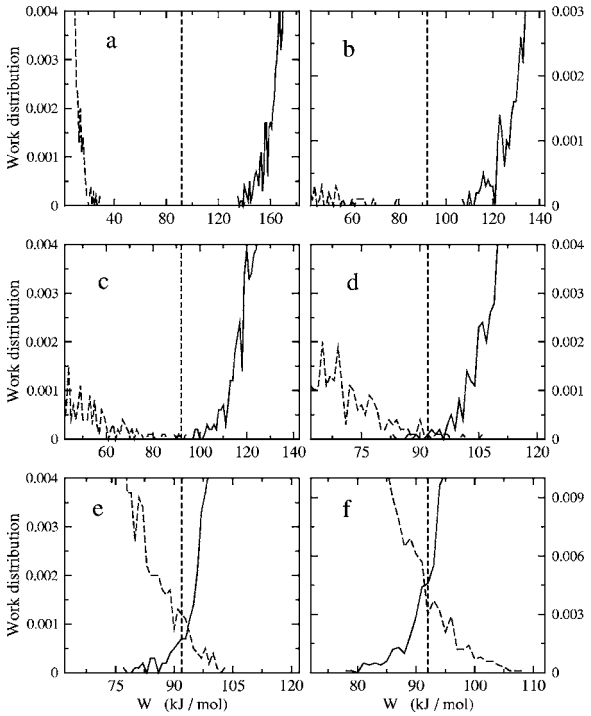

FIG. 5. Zoomed view (from Fig. 1) of the $P_f(W)$ and $P_b(-W)$ work distribution functions (solid and dashed lines, respectively) for various steering velocities (τ=10, 20, 30, 50, 100, and 200 ps from panel a to panel f). The vertical dashed lines show the value of ΔF obtained from the thermodynamic integration method.

Eq. (3) with no assumption on the work distributions is much better than those reported in Fig. 4 where the Gaussian shape assumption is used.

Although Fig. 5 furnishes a clear and quite conclusive numerical demonstration of the validity of the CE for NH molecular dynamics, the test of the CE we provide above is essentially based on a specific and very limited aspect of the equation, namely, that $W_x=\Delta F$. CE actually implies much more than this. In fact, Eq. (3) (and our specific application to SMD simulations), if physically true, must hold for any W. We can thus in principle recover $P_b(-W)$ [or $P_f(W)$] from the knowledge of the only quantities $P_f(W)$ [or $P_b(-W)$] and ΔF. We report this test in Fig. 6 for the steering time τ=200 ps. The agreement between the (forward or backward) work distribution as observed in the simulations and the one derived from its counterpart (backward or forward) via CE is very good, demonstrating numerically the validity beyond any reasonable doubt of the CE in the context of NH SMD simulations. The noise observed in the retrieved work distributions is due to the unavoidable poor statistics in the tails of the original work distributions. As previously noted, the distribution $P_b(-W)$ at τ=200 ns has an unexpected non-Gaussian character compared to the seemingly Gaussian shape of the corresponding $P_f(W)$ distribution. Nonetheless, as shown in Fig. 6, we were able to reconstruct an important part of the non-Gaussian backward distribution using the nearly Gaussian distribution of the forward process. This result points to the following conclusion: $P_f(W)$ is not Gaussian in its left tail, i.e., there where the body of the backward work distribution $P_b(-W)$ is carved.[22] Correspondingly, $P_b(-W)$ is approximately Gaussian only in its right tail, i.e.,

Downloaded 12 Nov 2012 to 150.217.154.21. Redistribution subject to AIP license or copyright; see http://jcp.aip.org/about/rights_and_permissions

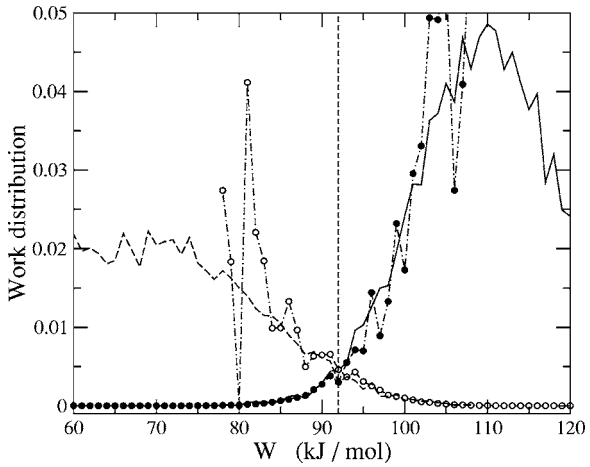

FIG. 6. $P_f(W)$ and $P_b(-W)$ work distribution functions (solid and dashed lines, respectively) for the steering velocity corresponding to $\tau=200$ ps. The open circled line is the backward work distribution obtained from the forward work distribution via CE. The full circled line is the forward work distribution obtained from the backward work distribution via CE.

for processes ending up, in average, with a successful reforming of the α-helix. This remarkable intertwined behavior of the forward and backward work distributions is compactly and elegantly accounted for by the CE.

IV. CONCLUSIONS

In the present study we provide a theoretical proof and numerical tests of the CE in the context of constant volume, constant temperature steered molecular dynamics simulations where the Nosé-Hoover thermostat is used. The generalization of the CE to Nosé-Hoover dynamical systems (not necessarily Markovian), along with the previous generalization provided by Evans for the isokinetic ensemble,[8] strengthens the idea[8] that the Jarzynski equality and the CE have general validity, both being a manifestation of the fluctuation theorem.[27]

In order to numerically verify the CE, tests on an isolated decaalanine peptide at finite temperature have been performed. Although the CE adapted to Gaussian work distributions [Eqs. (6) and (7)] does not yield satisfactory results for the unfolding and (especially) folding of decaalanine, the use of the CE without any assumption on the shape of the work distributions [Eq. (3)] allows to recover very precisely the exact folding/unfolding free energy. These results (i) show that the dynamics of decaalanine is far from being Markovian and (ii) provide a convincing numerical test of the validity of the CE for non-Markovian systems. We have also shown that the left tail of the forward work distribution is a crucial feature. This is so since it is in the left tail that, according to the CE, the shape of the backward work distribution is carved. For the same reasons, particular importance is also to be ascribed to the right tail of the backward work distribution. In the behavior of the tails of the work distributions we find not only a great deal of thermodynamical information but also valuable clues about the dynamical regime at the equilibrium typical of the underlying reaction coordinate.

From a practical standpoint, the CE expressed in terms of work distribution functions [Eq. (3)] cannot be applied, as such, for reconstructing the whole free energy profile along a given reaction path. As a matter of fact the CE allows to recover only free energy differences between two well defined macrostates. A full reconstruction of the free energy profile would require to split the interval of the reaction coordinate into several segments, where the CE machinery is applied independently. The determination of the whole free energy profile using one set of trajectories alone would be possible if the forward and backward transformations can be described by a Markovian process. However, as we have shown and discussed in the present report, this is not true for decaalanine and probably it is not true in general for biomolecules.

Finally, we stress that using the CE approach for estimating free energy differences in large biomolecular systems, though computationally expensive, could be made feasible exploiting the inherent parallelizability of the method.

ACKNOWLEDGMENTS

This work was supported by the Italian Ministero dell'Istruzione, dell'Università e della Ricerca and by the European Union (Grant No. RII3-CT-2003-506350).

APPENDIX A: PROOF OF EQUATION (9)

The proof of Eq. (9) proceeds as follows. Since the dynamics is deterministic, the probability ratio of the $A\rightarrow B$ and $A\leftarrow B$ transformations is simply given by the ratio between the number of initial points of the $A\rightarrow B$ process and the number of initial points of the time-reversal $A\leftarrow B$ process:

$$\frac{p[A(\mathbf{x}(0))\rightarrow B(\mathbf{x}(\tau))]}{p[A(\mathbf{x}(0))\leftarrow B(\mathbf{x}(\tau))]}=\frac{p[A(\mathbf{x}(0))]\delta\mathbf{x}(0)}{p[B(\mathcal{M}\mathbf{x}(\tau))]\mathcal{M}\delta\mathbf{x}(\tau)}, \tag{A1}$$

where $\mathcal{M}$ is the time-reversal operator such that $\mathcal{M}(\mathbf{q},\mathbf{p})=(\mathbf{q},-\mathbf{p})$. In the previous equation $\delta\mathbf{x}(0)$ and $\delta\mathbf{x}(\tau)$ are the volume elements of the phase space at the points $\mathbf{x}(0)$ and $\mathbf{x}(\tau)$, respectively. $p[A(\mathbf{x}(0))]$ and $p[B(\mathcal{M}\mathbf{x}(\tau))]$ are the equilibrium probabilities of the states $\mathbf{x}(0)$ and $\mathcal{M}\mathbf{x}(\tau)$. Since the equilibrium probability of a phase space state is independent on the sign of the momenta, the time-reversal operator does not affect the probability at the denominator, i.e., $p[B(\mathcal{M}\mathbf{x}(\tau))]=p[B(\mathbf{x}(\tau))]$. For the time-reversal trajectory, the volume element $\mathcal{M}\delta\mathbf{x}(\tau)$ is related to the volume element $\mathcal{M}\delta\mathbf{x}(0)$ through the Jacobian $J=\exp(-\int_0^\tau\nabla_\mathbf{x}\cdot\dot{\mathbf{x}}dt)$ of the transformation $\mathcal{M}\delta\mathbf{x}(0)\leftarrow\mathcal{M}\delta\mathbf{x}(\tau)$,

$$\mathcal{M}\delta\mathbf{x}(0)=\exp\left(-\int_0^\tau\nabla_\mathbf{x}\cdot\dot{\mathbf{x}}\,dt\right)\mathcal{M}\delta\mathbf{x}(\tau). \tag{A2}$$

Substituting Eq. (A2) into Eq. (A1) and exploiting the invariance of the phase space volume elements upon application of the time-reversal operator, i.e., $\mathcal{M}\delta\mathbf{x}=\delta\mathbf{x}$, we recover Eq. (9).

Downloaded 12 Nov 2012 to 150.217.154.21. Redistribution subject to AIP license or copyright; see http://jcp.aip.org/about/rights_and_permissions

APPENDIX B: CROOKS EQUATION FOR SMD SIMULATIONS USING THE NOSÉ-HOOVER CHAIN ALGORITHM

The demonstration of the CE for the case of a chain of M NH thermostats whose inertial factors are $M_{\eta_1}, M_{\eta_2}, \ldots, M_{\eta_M}$ follows the guideline we have described in Sec. II C. The substantial difference occurs in the equations of motion that in the case of the NH chain algorithm[20,21] coupled to a guiding potential are

$$\begin{aligned}
\dot{q}_i &= \frac{\partial H_0}{\partial p_i}, \\
\dot{p}_i &= -\frac{\partial H_0}{\partial q_i} - \frac{\partial V(\zeta,t)}{\partial q_i} - \dot{\eta}_1 p_i, \\
\dot{\eta}_k &= \frac{p_{\eta_k}}{M_{\eta_k}}, \quad k = 1, \ldots, M, \\
\dot{p}_{\eta_1} &= \sum_{i=1}^{3N} \frac{p_i^2}{m_i} - 3N\beta^{-1} - \frac{p_{\eta_2}}{M_{\eta_2}} p_{\eta_1}, \\
\dot{p}_{\eta_k} &= \frac{p_{\eta_{k-1}}^2}{M_{\eta_{k-1}}} - \beta^{-1} - \frac{p_{\eta_{k+1}}}{M_{\eta_{k+1}}} p_{\eta_k}, \quad k = 2, \ldots, M-1, \\
\dot{p}_{\eta_M} &= \frac{p_{\eta_{M-1}}^2}{M_{\eta_{M-1}}} - \beta^{-1}.
\end{aligned} \tag{B1}$$

Combining the equations of motion reported above with Eq. (16), we recover the analog of Eq. (18),

$$\begin{aligned}
Q_{AB} = &-3N\beta^{-1} \int_0^\tau \dot{\eta}_1 \, dt - \beta^{-1} \sum_{k=2}^{M} \int_0^\tau \dot{\eta}_k \, dt \\
&+ \sum_{k=1}^{M} \frac{p_{\eta_k}^2(0) - p_{\eta_k}^2(\tau)}{2M_{\eta_k}}.
\end{aligned} \tag{B2}$$

It is easy to prove that the compressibility of the system [analog of Eq. (19)] is

$$\nabla_{\mathbf{x}} \cdot \dot{\mathbf{x}} = -3N\dot{\eta}_1 - \sum_{k=2}^{M} \dot{\eta}_k. \tag{B3}$$

Combining Eqs. (B2) and (B3), we get the analog of Eq. (20),

$$\int_0^\tau \nabla_{\mathbf{x}} \cdot \dot{\mathbf{x}} \, dt = \beta Q_{AB} + \beta \sum_{k=1}^{M} \frac{p_{\eta_k}^2(\tau) - p_{\eta_k}^2(0)}{2M_{\eta_k}}. \tag{B4}$$

Finally, for a system coupled to a NH chain of thermostats, the ratio between the equilibrium probabilities $p[A(\mathbf{x}(0))]$ and $p[B(\mathbf{x}(\tau))]$ is [analog of Eq. (21)]:

$$\begin{aligned}
\frac{p[A(\mathbf{x}(0))]}{p[B(\mathbf{x}(\tau))]} = &\exp\left[\beta \sum_{k=1}^{M} \frac{p_{\eta_k}^2(\tau) - p_{\eta_k}^2(0)}{2M_{\eta_k}}\right] \\
&\times \exp[\beta(H(\tau) - H(0) - \Delta F)].
\end{aligned} \tag{B5}$$

Upon substitution of Eqs. (B5), (B4), and (12) into Eq. (9), we recover the CE [Eq. (22)].

[1] C. Jarzynski, Phys. Rev. Lett. **78**, 2690 (1997).
[2] C. Jarzynski, Phys. Rev. E **56**, 5018 (1997).
[3] G. E. Crooks, J. Stat. Phys. **90**, 1481 (1998).
[4] More precisely, the CE is a relation that holds for each single dissipative transformation, while the JE involves an ensemble average (over all possible transformations) of a function of the work W done on the system, i.e., $\langle \exp(-\beta W) \rangle$.
[5] C. Jarzynski, J. Stat. Mech.: Theory Exp. 2004, P09005.
[6] M. P. Allen and D. J. Tildesley, *Computer Simulation of Liquids* (Clarendon, Oxford, 1987).
[7] G. E. Crooks, Phys. Rev. E **61**, 2361 (2000).
[8] D. J. Evans, Mol. Phys. **101**, 1551 (2003).
[9] D. J. Evans and D. J. Searles, Adv. Phys. **51**, 1529 (2002).
[10] J. Liphardt, S. Dumont, S. B. Smith, I. Tinoco, and C. Bustamante, Science **296**, 1832 (2002).
[11] D. Collin, F. Ritort, C. Jarzynski, S. B. Smith, I. Tinoco, and C. Bustamante, Nature (London) **437**, 231 (2005).
[12] R. D. Astumian, Am. J. Phys. **74**, 683 (2006).
[13] E. G. D. Cohen and D. Mauzerall, J. Stat. Mech.: Theory Exp. 2004, P07006.
[14] S. Park and K. Schulten, J. Chem. Phys. **120**, 5946 (2004).
[15] G. Hummer, J. Chem. Phys. **114**, 7330 (2001).
[16] J. Gore, F. Ritort, and C. Bustamante, Proc. Natl. Acad. Sci. U.S.A. **100**, 12564 (2003).
[17] I. Kosztin, B. Barz, and L. Janosi, J. Chem. Phys. **124**, 064106 (2006).
[18] W. G. Hoover, Phys. Rev. A **31**, 1695 (1985).
[19] W. G. Hoover, Phys. Rev. A **34**, 2499 (1986).
[20] G. J. Martyna, Phys. Rev. E **50**, 3234 (1995).
[21] M. E. Tuckerman, B. J. Berne, G. J. Martyna, and M. L. Klein, J. Chem. Phys. **99**, 2796 (1993).
[22] C. Jarzynski, Phys. Rev. E **73**, 046105 (2006).
[23] M. A. Cuendet, Phys. Rev. Lett. **96**, 120602 (2006).
[24] S. Park, F. Khalili-Araghi, E. Tajkhorshid, and K. Shulten, J. Chem. Phys. **119**, 3559 (2003).
[25] G. E. Crooks, Phys. Rev. E **60**, 2721 (1999).
[26] M. E. Tuckerman, Y. Liu, G. Ciccotti, and G. J. Martyna, J. Chem. Phys. **115**, 1678 (2001).
[27] D. J. Evans, E. G. D. Cohen, and G. P. Morriss, Phys. Rev. Lett. **71**, 2401 (1993).
[28] J. Hénin and C. Chipot, J. Chem. Phys. **121**, 2904 (2004).
[29] C. Chipot and J. Hénin, J. Chem. Phys. **123**, 244906 (2005).
[30] A. Mackerell, D. Bashford, M. Bellot *et al.*, J. Phys. Chem. B **102**, 3586 (1998).
[31] P. Procacci, T. A. Darden, E. Paci, and M. Marchi, J. Comput. Chem. **18**, 1848 (1997).

Downloaded 12 Nov 2012 to 150.217.154.21. Redistribution subject to AIP license or copyright; see http://jcp.aip.org/about/rights_and_permissions